state peak exhibits a fluctuating background without enough consistency with angle to permit specific assignments.

Additional groups of particles discriminated as alphas are observed for $E_\alpha = 3.21 \pm 0.03$ Mev at 90° and $E_\alpha = 3.10 \pm 0.03$ Mev at 101° (Figs. 2 and 3). We have been unable to assign these to plausible contaminations of the natural boron target on a thick tantalum backing. If assigned to $B^{11}(d,\alpha)Be^9$, they correspond to states at 4.59 and 4.41 Mev in Be^9. These might correspond to the broad 4.9-Mev level reported in reference 3, although it seems unlikely that such groups would have been missed in the high-resolution work of reference 1. We suggest instead that they are probably spectroscopic[6] "ghosts" of the adjacent $O^{16}(d,p)O^{17}$ peaks. Such a ghost appears, for example, on the high-energy side of the $C^{12}(d,p)C^{13}$ peak at both 90° and 101°. The pulses of these peaks are discriminated in the surplus above the alpha channels and thus recorded as protons, though with more careful discrimination the ghost pulses have ordinarily been found between the larger pulses of the direct proton peak and the smaller alpha pulses, the ghost protons presumably having lost energy on scattering from the inner (small-radius) wall of the deflection chamber. Apparently in the energy region of the peaks in question the ghost pulses happen to fall just in the alpha channels, for they do not appear elsewhere. We have thus not indicated levels corresponding to these peaks in the energy level diagram shown in the small insert of Fig. 1, even as broken lines, but further investigation of the region above 4 Mev is surely needed. The deuteron scattering edge at an equivalent of about 4.6 Mev in Be^9 prevented our observation of states at higher energies.

PHYSICAL REVIEW VOLUME 99, NUMBER 1 JULY 1, 1955

Photofission of U^{238}

L. KATZ, T. M. KAVANAGH, A. G. W. CAMERON, E. C. BAILEY, AND J. W. T. SPINKS
University of Saskatchewan, Saskatoon, Canada

(Received February 7, 1955)

Chemical separation of the products resulting from photofission at various maximum bremsstrahlung energies E_0 of U^{238} serve to define the 3-dimensional yield surface $S(Y,A,E_0)$. An analysis of this surface by the photon difference method established the 3-dimensional photofission cross section surface $S(\sigma,A,h\nu)$. The peak-to-valley cross section ratio (asymmetric to symmetric fission) is examined in some detail and the results are combined with high-energy photofission data from the literature to extend our calculations and analysis to 300 Mev.

INTRODUCTION

PHOTOFISSION, the fission process induced by nuclear absorption of electromagnetic energy, has been the subject of a number of investigations. For a discussion of the earlier work in this field the review article by Spencer and Ford[1] may be consulted. The early work indicated that the cross section for photofission, $\sigma_{\gamma f}$, increased from zero at the threshold to a maximum value at about 14 Mev and decreased thereafter with increasing energy. This cross-section shape is similar to that found for other photonuclear reactions and is termed the "giant" resonance cross section.[2-4] Recent work by Duffield and Huizenga[5] has shown that this giant photofission cross section in U^{238} has a peak value of about 0.18 barn and a width of 7 Mev at half-maximum.

An examination of the photofission yield as a function of mass number, at a given photon energy shows it to have the usual double humped mass distribution. Schmitt and Sugarman[6] have studied the shape of such mass-yield curves from natural uranium when irradiated with bremsstrahlung of maximum energy $E_0 = 7$, 10, 16, 21, 48, 100, and 300 Mev. Since these curves contain contributions from all photons in the spectrum whose energy is above the photofission threshold (5.1 Mev in uranium)[7] the direct interpretation of their curves is somewhat difficult.

Richter and Coryell[8] have given photofission mass-yield curves for natural uranlum at energies $E_0 = 10$ and 16 Mev. Hiller and Martin[9] published a similar curve for thorium obtained with bremsstrahlung of 69-Mev peak energy.

In line with other photonuclear investigations being carried out in our laboratory we have studied the photofission process in natural uranium as a function of

[1] R. W. Spencer and G. P. Ford, Ann. Rev. Nucl. Sci. **2**, 400 (1953).
[2] Johns, Katz, Douglas, and Haslam, Phys. Rev. **80**, 1062 (1950).
[3] B. C. Diven and G. M. Almy, Phys. Rev. **80**, 407 (1950).
[4] Montalbetti, Katz, and Goldemberg, Phys. Rev. **91**, 659 (1953).
[5] R. B. Duffield and J. R. Huizenga, Phys. Rev. **89**, 1042 (1953).
[6] R. A. Schmitt and N. Sugarman, Phys. Rev. **95**, 1260 (1954).
[7] Koch, McElhinney, and Gasteiger, Phys. Rev. **77**, 329 (1950).
[8] H. C. Richter and C. D. Coryell, Phys. Rev. **95**, 1550 (1954).
[9] D. M. Hiller and D. S. Martin, Jr., Phys. Rev. **90**, 581 (1953).

energy from threshold to 24 Mev. Sufficient measurements were taken to establish the shape of the mass-yield surface as a function of bremsstrahlung energy E_0. This surface will be designated by $S(Y,A,E_0)$ where $Y(E_0,A)$ represents the yield of mass number A resulting from a given irradiation with photons whose maximum bremsstrahlung energy is E_0. A cut through this surface at constant mass number A corresponds to the yield of this mass chain in photofission as the energy E_0 is varied. The curve so obtained is similar to the usual yield curve in photonuclear reactions and may be analyzed by the photon difference method of Katz and Cameron[10] to yield the corresponding cross section. This cross section may be written $(\sigma_{\gamma f}(h\nu))_A$. It has the "resonance" shape characteristic of photonuclear reactions and obviously must be interpreted as the cross section leading to the mass chain A in the photofission process induced by photons of energy $h\nu$.

It is now possible, with the aid of the $(\sigma_{\gamma f}(h\nu))_A$ curves, to construct a three-dimensional surface $S(\sigma,A,h\nu)$. A cut through this surface at constant $h\nu$ results in a $\sigma-A$ curve which is readily seen to be the mass yield curve which would be obtained with monochromatic photons. For this reason the $S(\sigma,A,h\nu)$ surface is of particular interest in the study of photofission. The area under the $\sigma-A$ curve obtained by cutting this surface at constant energy $h\nu$ is the total photofission cross section at that energy. It will be shown that this curve has the double humped shape characteristic of fission yield curves obtained with particle excitation.

To within the accuracy of our measurements the mass chain 115 falls in the trough of the $S(\sigma,A,h\nu)$ surface so that $(\sigma_{\gamma f})_{115}$ can be taken as representing the cross section for symmetric fission. The mass chain 139 falls near the top of the higher mass peak and can be taken as representing the cross section for asymmetric fission. The ratio

$$R(h\nu)=(\sigma_{\gamma f})_{139}/(\sigma_{\gamma f})_{115} \quad (1)$$

is then of particular interest and is discussed at some length.

EXPERIMENTAL PROCEDURE

Thirteen-gram samples of uranyl nitrate, enclosed in a cadmium container, were irradiated in the betatron beam 28 cm in front of the electron target from which the bremsstrahlung beam originated. The dose was monitored by a 100 "r" Victoreen chamber placed in the center of an 8-cm cube of Lucite and positioned 62 cm from the electron target. After applying corrections for inverse square divergence of the beam and the angular dependance of the intensity over the finite angle subtended by the sample at the electron target, it was possible to reduce each irradiation to the same dose rate. Irradiations used lasted 10 minutes at high energy and 2 hr at low energy ($\sim$15 000 roentgens per irradiation).

The desired nuclides were isolated for counting by chemical methods and were deposited by filtration on 1-inch diameter filter papers ($\sim$9 mg/cm^2). The chemical procedures followed were those outlined in the Plutonium Project Report[11] with slight modifications particularly in the cadmium procedure to include a tin scavenging step. The filter papers containing the activity were mounted in holders between two plastic films about 1 mg/cm^2 thick and were counted in an automatic counting device. This automatic counter was built to accommodate up to 11 samples and one standard source whose activity could be measured in sequence. In most cases decay curves were followed through several half-lives with a recorded count of 6000 disintegrations for each point on the decay curves.

Since preliminary measurements established that the $S(Y,A,E_0)$ surface as a function of E_0 is reasonably smooth, mass yield curves were taken only at betatron energies of 12, 18, and 22 Mev. Yield measurements were carried out on 12 fission product nuclides with barium separated in each case so that the activity of Ba^{139} could be used as a control activity. The 3 mass-yield curves, coupled with measurements of the yields of Cd^{115} and Ba^{139} at $\sim$1 Mev intervals to 24 Mev, served to define the $S(Y,A,E_0)$ surface.

COMPUTATIONS

Usually, in fission yield analysis one is not concerned with the measurement of individual nuclides but rather with the total yield of each beta decay chain. For this reason computations should be based on the yield of stable isotopes at the end of the chains. However, negligable error is involved if isotopes one or two places removed from the stable nuclide are used. Since the early members of a decay chain are largely very short-lived, a two-stage decay equation will usually represent the yields with sufficient accuracy. That is, the parent of the nuclide being counted may be considered as a primary fission product and the yield $Y(E_0,A)$ of mass chain A in atoms per roentgen of irradiation per atom of U^{238} is given by

$$Y(E_0,A)=\frac{\lambda_2 N_2(\lambda_2-\lambda_1)}{\lambda_2\phi N_0} \times\left[(1-e^{-\lambda_1 t_R})e^{-\lambda_1 t}-\frac{\lambda_1}{\lambda_2}(1-e^{-\lambda_2 t_R})e^{-\lambda_2 t}\right]^{-1}, \quad (2)$$

where λ_1, λ_2 = the decay constants of the parent and daughter nuclides respectively; $\lambda_2 N_2$ = activity in counts/min of the daughter at time of separation from parent (corrected for counting efficiency and corrected to 100 percent chemical recovery); ϕ = x-ray intensity averaged over the uranium sample in roentgens per minute; N_0 = number of uranium atoms in the sample

[10] L. Katz and A. G. W. Cameron, Can. J. Phys. **29**, 518 (1951).

[11] D. C. Coryell and N. Sugarman, *Radiochemical Studies; The Fission Products* (McGraw-Hill Book Company, Inc., New York, 1951), National Nuclear Energy Series Plutonium Project Record, Vol. 9, Div. IV.

TABLE I. Yield of mass chains 115 and 139 in radioactive nuclei per atom U^{238} per roentgen of irradiation.

E_0 Mev	Yield $A=115$	$A=139$
8		0.37×10^{-19}
10		1.15
12	0.36×10^{-20}	2.29
13	0.68	2.85
13.5	0.74	3.53
14	1.12	3.82
15	1.35	4.83
16	1.88	4.88
18	2.97	5.45
20		6.02
20.2	3.65	6.28
22	4.22	6.23
22.5	3.93	6.47
23	4.97	
23.5		6.28
24	4.77	6.47

from which chemical separation is made; t_R = duration of irradiation; and t = decay time from end of irradiation to time of separation from the parent.

This yield is related to the cross section for photofission by the equation

$$Y(E_0,A)=\int_0^{E_0} P(h\nu,E_0)(\sigma_{\gamma f}(h\nu))_A dh\nu, \qquad (3)$$

where $P(h\nu,E_0)$ is the number of photons of energy $h\nu$ per roentgen of irradiation, falling per cm^2 of sample when the maximum bremsstrahlung energy is E_0, per Mev energy interval.

If the isotope being counted had a short-lived β-emitting daughter, then a correction was applied for the growth of this daughter subsequent to chemical separation.

The decay schemes for the 12 fission-product nuclides separated chemically for our mass-yield studies were taken from the Tables of Isotopes by Hollander, Pearlman, and Seaborg.[12] These tables contain the most recent survey of the literature and no pertinent new results on the 12 isotopes have appeared since their publication.

Corrections for self-absorption are very small since the samples were all less than 8 mg/cm^2 thick. They were calculated according to the methods of Baker and Katz.[13] Corrections for external absorption were applied under the assumption that it is exponential with the absorption coefficient given by Eq. (6) of reference 13. To obtain a backscattering correction, the data of Engelkemeir *et al.*[14] and Yaffe[15] were combined. This gave the percent backscattering from our filter paper as a function of beta energy. This correction was always less than 10 percent.

[12] Hollander, Pearlman, and Seaborg, Revs. Modern Phys. **25**, 469 (1953).
[13] R. G. Baker and L. Katz, Nucleonics **II**, No. 2, 14 (1953).
[14] Engelkemeir, Seiler, Steinberg, and Winsberg, paper 9, reference 11.
[15] L. Yaffe, *Conference on Absolute Beta Counting*, Preliminary Report No. 8 (National Research Council, Washington, D. C., 1950).

The geometric efficiency of the counting system was determined by our usual method of irradiating a copper disk in the betatron beam under standard conditions and counting the induced Cu^{62} activity. Comparison of this to the known activity for the sample in 4π geometry[10] then gave the geometric efficiency. Because of the size of the uranium sample it was necessary to apply one further correction. Suppose $I_0(h\nu)$ is the photon intensity of energy $h\nu$ falling on the sample surface, then the intensity at a distance x within the sample is

$$I_0\left(\frac{a}{a+x}\right)^2 e^{-\mu\rho x}, \qquad (4)$$

where a is the distance of the sample front from the electron target, $\mu(h\nu)$ is the mass absorption coefficient of uranyl nitrate, and ρ is the sample density. The average intensity for a sample of length b is

$$\bar{I}=\frac{I_0}{b}\int_0^b \frac{e^{-\mu\rho x}}{(1+x/a)^2}dx. \qquad (5)$$

Since in our case $a=28$ cm and $b=5.5$ cm, we can assume $x/a<1$ over the region of integration. This approximation shows the dependence of I/I_0 on $(h\nu)$ is primarily through the relation $(1-e^{-\mu\rho b})/\mu\rho b$. Though μ is a strong function of $h\nu$, the variation of $\bar{I}/I_0$ with energy is less than 2 percent over the energy range involved in this work. Calculation gives $\bar{I}=0.70I_0$ and show it to be insensitive to slight variations in ρ from sample to sample.

The total yield of fissioning nuclides at a betatron operating energy E_0, per irradiated U^{238} nucleus per roentgen of irradiation is given by

$$Y(E_0)=\int_0^{238} Y(E_0,A)dA. \qquad (6)$$

We can now define the total photofission cross section by the equation

$$Y(E_0)=\int_0^{E_0} P(h\nu,E_0)\sigma_{\gamma f}(h\nu)dh\nu, \qquad (7)$$

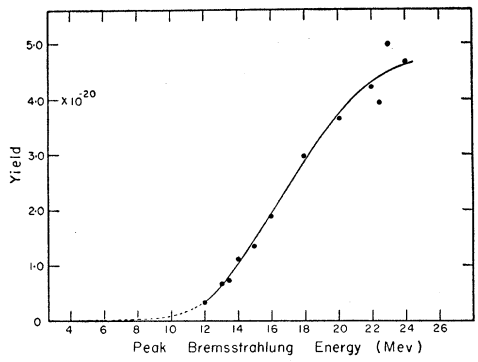

FIG. 1. Yield of mass chain 115 resulting from photofission of U^{238} as indicated by the yield of the 54-hr Cd^{115} beta-ray activity. The yield is expressed in nuclei of mass 115 per irradiated U^{238} nucleus per roentgen of irradiation.

where $P(h\nu,E_0)$ has been already defined and $\sigma_{\gamma f}(h\nu)$ is the cross section for causing fission by photons of energy $h\nu$. Substituting $Y(E_0,A)$ from Eq. (3) into (6) and inverting the order of integration, we find

$$\sigma_{\gamma f}(h\nu)=\int_0^{238}(\sigma_{\gamma f}(h\nu))_A dA. \quad (8)$$

EXPERIMENTAL RESULTS

The measured yields of mass chains 115 and 139 (Cd^{115} and Ba^{139}) in nuclei per U^{238} nucleus per roentgen of irradiation as a function of betatron operating energy E_0 are summarized in Table I. Owing to low yield, no measurements were obtained below 12 Mev on mass chain 115 and below 8 Mev on mass chain 139. These results are plotted in Figs. 1 and 2 with the dashed parts of the curves representing a smooth extrapolation of the experimental data to low energy.

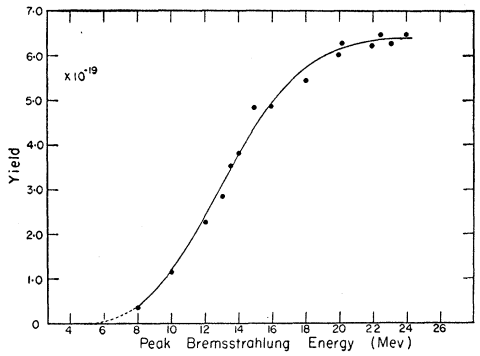

FIG. 2. Yield of mass chain 139 resulting from photofission of U^{238} as indicated by the yield of 85-min Ba^{139}. The yield is expressed in nuclei of mass 139 per irradiated U^{238} nucleus per roentgen of irradiation.

The results of our measurements on the yield of 12 mass chains at betatron operating energies of 12, 18, and 22 Mev are summarized in Table II. These yields are expressed in nuclei in each mass chain per irradiated U^{238} nucleus per roentgen of irradiation. We estimate the values given in this table to be accurate to within ± 25 percent and the relative dispersion among the values plotted in Figs. 1 and 2 to be considerably less, probably 10 percent.[16] The yields are plotted in Figs. 3, 4, and 5 as circles. It was found that in all cases reflection of these points about mass 117.5 resulted in a smooth curve. This corresponds to the emission on an average of 3 neutrons per fission, in good agreement with the measurements of other workers.[6,8] The reflected points are indicated by crosses in the three figures. Few points were available for the 12-Mev curve because of the low activities of the longer-lived fission-fragment nuclides.

[16] An estimate in this relative scattering in our yield measurements can be obtained from an examination of Figs. 1 and 2. There is good reason to expect that experimental points should be on a smooth curve, and dispersion of the points from such a smooth curve indicates the accuracy to which measurements could be repeated.

TABLE II. Mass yields at constant E_0 in radioactive nuclei per atom U^{238} per roentgen of irradiation.

Mass No.	Nuclide measured	Yield $E_0=12$ Mev	$E_0=18$ Mev	$E_0=22$ Mev
77	39 hr As^{77}			0.06×10^{-19}
83	2.4 hr Br^{83}	0.15×10^{-19}	0.53×10^{-19}	0.61
89	54 day Sr^{89}		4.9	5.3
97	17 hr Zr^{97}		7.1	7.4
99	67 hr Mo^{99}		6.1	6.9
103	40 day Ru^{103}			3.9
105	4.5 hr Ru^{105}	1.0	2.3	2.6
111	7.5 day Ag^{111}		0.23	0.36
115	54 hr Cd^{115} + 43 day Cd^{115m}	0.036	0.29	0.43
138	30 min Cs^{138}		5.9	6.9
139	85 min Ba^{139}	2.4	5.6	6.3
143	33 hr Ce^{143}		5.3	5.8

This curve was drawn to have essentially the same shape as the 18- and 22-Mev curves. The double humped shape of the 18- and 22-Mev curves is quite well defined by the experimental points, and while no special attempt was made to measure the fine structure reported at masses 100 and 134[8,17,18] the high yields of Mo^{99} and Zr^{97} may be taken to indicate that it has been detected in our experiments. It will also be noted that mass 111 falls slightly below mass 115 in the 18- and 22-Mev curves. This is not in agreement with other photofission results and may be due to the difference in the absolute normalization of the mass 115 activation curve.

Peak-to-valley ratio of the fission yield curves is obtained directly from Figs. 1 and 2. This ratio is shown as curve A of Fig. 6. Schmitt and Sugarman reported values of 200, 38, 23, and 20 for this ratio at $E_0=10$, 16, 21 and 22 Mev, respectively. These values are somewhat higher than those found by us at corresponding energies, which are 150, 25, 15, and 14. The disagreement is within the combined error of both sets of measurements and is likely due to the absolute normalization of the

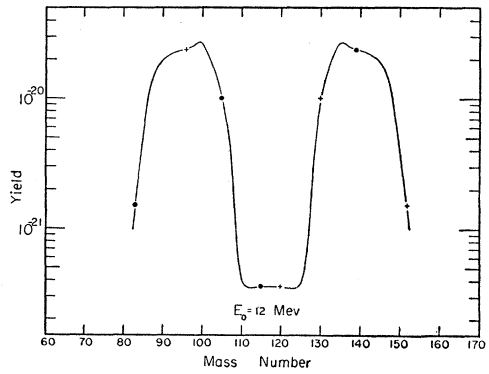

FIG. 3. Yield of mass chains 83, 105, 115, and 139 at a betatron operating energy of 12 Mev. The measurements are indicated by the circles and reflection of these about mass 117.5 are indicated by crosses. The curve drawn through these points was made to correspond in shape to those shown in Figs. 4 and 5.

[17] Glendenin, Steinberg, Inghram, and Hess, Phys. Rev. **84**, 860 (1951).

[18] D. R. Wiles and C. D. Coryell, Phys. Rev. **96**, 696 (1954).

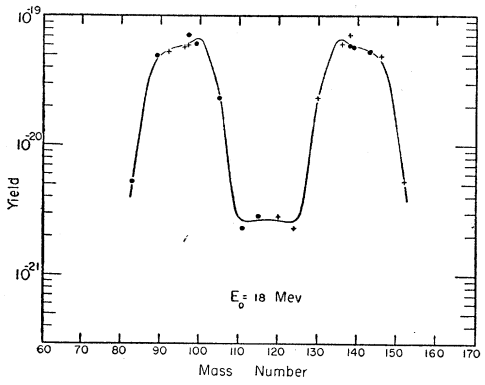

FIG. 4. Yield of mass chains 83, 89, 97, 99, 105, 111, 115, 138, 139, and 143 at a betatron operating energy of 18 Mev. The measurements are indicated by the circles and reflection of these about mass 117.5 are indicated by crosses.

mass 115 chain activation curve. The results of both investigations show a similar smooth variation of the peak-to-valley ratio with betatron operating energy. This is in strong disagreement with the results of Richter and Coryell[8] who obtained a value of 110 at $E_0=16$ Mev and predicted a sharp drop in this ratio just above 16 Mev.

In Fig. 7 we again show the peak-to-valley yield ratio, this time on a log-log plot. Our measurements are represented by the heavy line. The results of Schmitt and Sugarman[6] to 300 Mev are indicated by circles and those of Richter and Coryell[8] by crosses. The changing peak-to-valley ratio at high energy has been correctly interpreted by Schmitt and Sugarman[19] to indicate a tail on the $\sigma_{\gamma f}$ cross section. For the purpose of the analysis which will be carried out later our ratio has been extrapolated to high energy in agreement with the data of Schmitt and Sugarman. This extrapolation is indicated by the light solid line of Fig. 7.

Figures 1 to 6 serve to define the whole $S(Y,A,E_0)$ surface to 24 Mev. Intermediate points on the surface

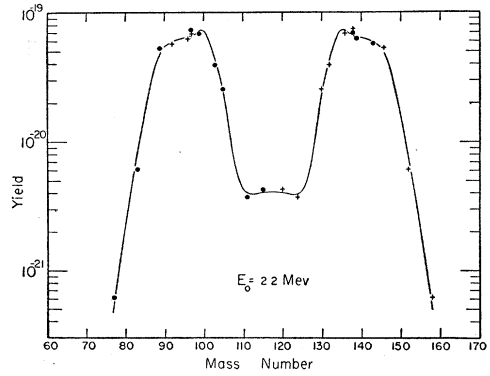

FIG. 5. Yield of mass chains 77, 83, 89, 97, 99, 103, 105, 111, 115, 138, 139, and 143 at a betatron operating energy of 22 Mev. The measurements are indicated by the circles and reflection of these about mass 117.5 are indicated by crosses.

[19] R. A. Schmitt and N. Sugarman, Phys. Rev. **89**, 1155 (1953).

were obtained, to within experimental accuracy by various cross plots of these 6 figures. This procedure naturally smooths over any fine structure detail, but does give the 3-dimensional shape of the yield surface in its broad outline.

ANALYSIS AND DISCUSSION OF EXPERIMENTAL RESULTS

Analysis of the data in Table I by the photon difference method[10] gave the photofission cross sections from threshold to 24 Mev leading to mass chains 115 and 139, that is $(\sigma_{\gamma f})_{115}$ and $(\sigma_{\gamma f})_{139}$. These cross sections are shown in Figs. 8 and 9 as a function of photon energy. The values above 24 Mev indicated in these curves were calculated by another method which will be discussed later.

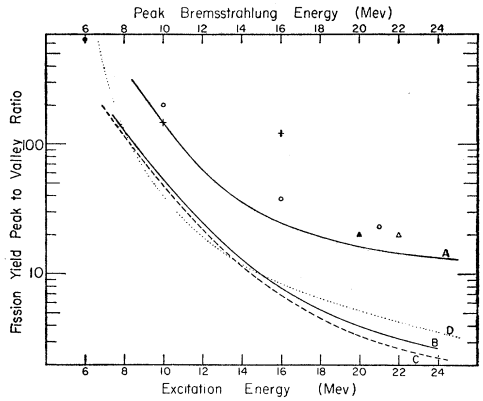

FIG. 6. Curve A: Ratio of mass 139 yield to mass 115 yield as a function of betatron operating energy (peak bremsstrahlung energy as shown on top scale). For comparison we have shown the ratio in similar measurements by Schmitt and Sugarman, reference 6 (open circles) and reference 19 (open triangle); by Richter and Coryell, reference 8 (crosses); and by Spencer, Table III, reference c (black triangle). Curve B: Ratio of photofission cross sections leading to mass chains 139 and 115 (asymmetric to symmetric fission) as a function of photon energy (bottom scale). Curve C: Asymmetric to symmetric fission yields *vs* energy of excitation as given by Hill and Wheeler, reference 21. This curve is based on the results of fission induced in various nuclides by energetic particles. Curve D: Similar to C according to Turkevich *et al.*, reference 22. Solid black circle gives ratio for thermal neutron fission of U^{235}.

The cross sections show the usual "resonance" shape characteristic of other photonuclear cross sections. $(\sigma_{\gamma f})_{115}$ reaches a maximum value of 0.73 millibarn at 18 Mev while $(\sigma_{\gamma f})_{139}$ has a maximum value of 6.8 millibarns at 14 Mev. Both cross sections have a width at half-maximum of about 9 Mev. The shift in the peak position of $(\sigma_{\gamma f})_{115}$ relative to $(\sigma_{\gamma f})_{139}$ towards higher energy by about 4 Mev is of some interest.[20]

Curve B of Fig. 6 shows the cross-section ratio $R=(\sigma_{\gamma f})_{139}/(\sigma_{\gamma f})_{115}$ as a function of photon energy. This ratio is of greater physical significance than curve A since it gives the probability ratio of asymmetric to symmetric fission as a function of nuclear excitation energy whereas curve A is the average of this ratio over

[20] Fowler, Jones, and Paehler, Phys. Rev. **88**, 71 (1952).

the bremsstrahlung spectrum. Hill and Wheeler[21] and Turkevich *et al.*[22] have drawn curves of peak-to-valley ratio against excitation energy by collecting the results of many workers on fission induced in various nuclides by energetic particles. Their results are shown as curves *C* and *D* respectively in Fig. 6. These are in excellent agreement with our results. In all cases the peak-to-valley ratio changes from approximately 150 at 8-Mev excitation to about 3 at 24-Mev excitation. (In the case of particle induced fission the excitation energy is of course the incident particle energy plus its binding energy to the target nucleus.)

It is of some interest to examine in greater detail the ratio discussed above. This examination is particularly meaningful since the present work gives the ratio for a single uranium isotope over a fairly extended energy range. It has been suggested[20] that a plot of $\ln R$ against

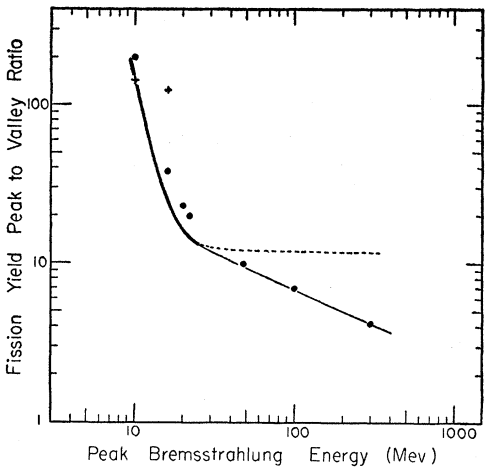

FIG. 7. Black solid line: Ratio of peak-to-valley yields taken from curve *A* of Fig. 6. Circles: Ratio of peak-to-valley yields to 300 Mev from reference 6. Light solid line: smooth extrapolation of our data to high energy. Crosses: Measurements of this ratio by Richter and Coryell, reference 8. Dashed line: Ratio which would have been obtained at high energy if symmetric and asymmetric cross-section curves had no tail beyond 24 Mev.

$(E-\Phi)^{-\frac{1}{2}}$ should yield a straight line, where R is defined above, E is the nuclear excitation energy, equal to $h\nu$ in our case, and Φ is a constant, probably the photofission threshold.[23] Fowler *et al.*[20] have collected the experimental ratios of many workers and using such a plot found a straight line to give the best fit. In Fig. 10 we

[21] D. L. Hill and J. A. Wheeler, Phys. Rev. **89**, 1102 (1953).
[22] Turkevich, Niday, and Tompkins, Phys. Rev. **89**, 552 (1953).
[23] There is some confusion as to the exact meaning of "photofission threshold." Energetically, since the U^{238} nucleus will undergo spontaneous fission, this threshold should be less than zero and we should take $\Phi=0$. On the other hand, from an experimental point of view there is some energy of excitation which is required to give a readily detectable fission rate (say one fission per hour). The exact energy assigned to this "experimental" threshold will depend only slightly on the apparatus sensitivity. Thus, in the case of U^{238}, measurements in our laboratory show that an increase in the sensitivity of the apparatus for determination of threshold by a factor of 10 lowers the "observed" threshold by less than 0.1 Mev. It can be argued that Φ should correspond to this "experimental" threshold, namely 5.1 Mev.

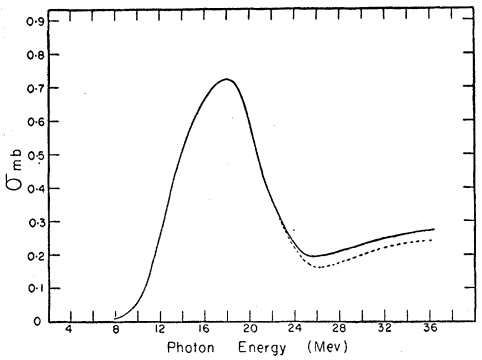

FIG. 8. Cross section for symmetric fission obtained from analysis of Fig. 1 by the photon difference method. The cross section above 24 Mev was obtained from the analysis of the ratio of Fig. 7 as outlined in the text. The dashed curve is obtained if the asymmetric cross section is assumed zero above 24 Mev.

show plots with $\Phi=0$ and 5.1 Mev, using our results from 12 to 24 Mev and using at lower energies the results obtained from neutron-induced fission in various isotopes of uranium. The results for neutron-induced fission are summarized in Table III. Our results were not felt to be sufficiently reliable below 12 Mev for this study.

For $\Phi=0$ a straight line is obtained; however, if we accept $\Phi=5.1$ we must conclude that there is a break in the curve at $h\nu=10$ Mev. If this break actually exists, one can suggest a number of reasons for it. First we notice that the break occurs at an energy where neutron emission followed by fission becomes energetically possible. The process of neutron emission may perhaps result in a changed value of R. Secondly, whatever the reason, one could suggest that there are two modes of symmetric fission and one mode of asymmetric fission. In this case we could write

$$R=\frac{(\sigma_{\gamma f})_{139}}{(\sigma_{\gamma f})_{115}'+(\sigma_{\gamma f})_{115}''}=\frac{R_1R_2}{R_1+R_2}, \tag{9}$$

where

$$R_1=(\sigma_{\gamma f})_{139}/(\sigma_{\gamma f})_{115}' \quad \text{and} \quad R_2=(\sigma_{\gamma f})_{139}/(\sigma_{\gamma f})_{115}''.$$

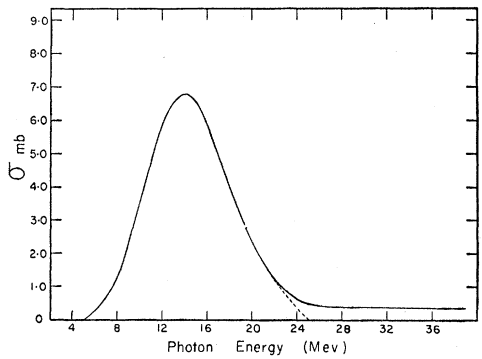

FIG. 9. Cross section for asymmetric fission obtained from analysis of Fig. 2 by the photon difference method. The cross section above 24 Mev was obtained from the analysis of the ratio of Fig. 7 as outlined in the text.

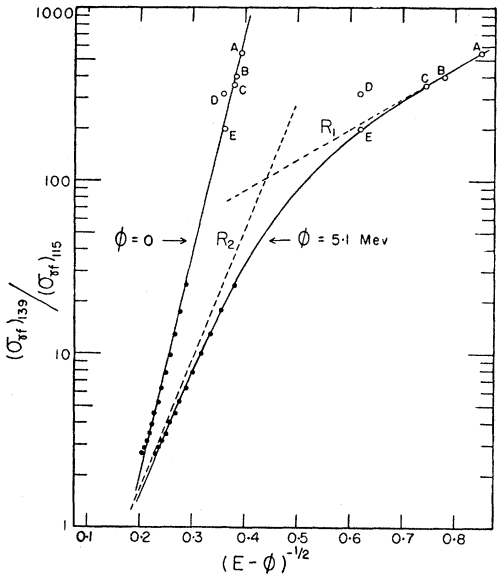

FIG. 10. Plots of the logrithm of the ratio of asymmetric to symmetric photofission cross sections as a function of $(E-\Phi)^{-\frac{1}{2}}$, where E is the excitation energy and Φ is a constant. Plots for two values of Φ are shown. Black points are values taken from curve B of Fig. 6 at 1-Mev intervals in the energy range of 12 to 24 Mev and the other points are listed in Table III; A reference a of Table III, B reference b, C and D reference c, and E reference d. For $\Phi=0$ the best fit straight line is drawn, and for $\Phi=5.1$ Mev the line drawn is $R_1R_2/(R_1+R_2)$, where R_1 and R_2 are the dashed straight lines as shown.

The primes distinguish between the two modes of symmetric fission. The solid line for $\Phi=5.1$ represents the expression $R_1R_2/(R_1+R_2)$, with R_1 and R_2 shown by the dashed straight lines in the diagram. To emphasize the agreement between our experimental data and this line, we have plotted points at 1-Mev intervals taken from the smooth curve of Fig. 6B. These procedures are entirely empirical and it is not clear whether any significance is to be attributed to the conclusions.

HIGH-ENERGY FISSION CROSS SECTION

It is possible to calculate the photofission cross section leading to symmetric and asymmetric fission in the energy region from 24 to 300 Mev with the aid of our cross section curves of Figs. 8 and 9, Schmitt and Sugarman's yield ratio as shown in Fig. 7 and the following analysis. According to Eq. (3) we can write the ratio of yields at bremsstrahlung energy E_0:

$$R(E_0)=\frac{\int_0^{E_0}P(h\nu,E_0)(\sigma_{\gamma f}(h\nu))_a dh\nu}{\int_0^{E_0}P(h\nu,E_0)(\sigma_{\gamma f}(h\nu))_s dh\nu}, \qquad (10)$$

where the subscripts a and s designate the cross sections for asymmetric and symmetric fission. For energies above 24 Mev, the cross sections are not expected to be strong functions of energy and we can write

$$R(E_0)=\frac{\int_0^{24}P\sigma_a dh\nu+\bar{\sigma}_a\int_{24}^{E_0}P dh\nu}{\int_0^{24}P\sigma_s dh\nu+\bar{\sigma}_s\int_{24}^{E_0}P dh\nu}, \qquad (11)$$

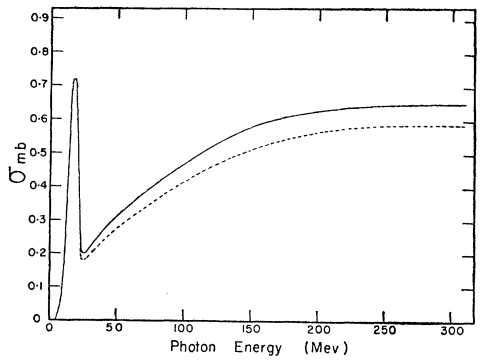

FIG. 11. Cross section for symmetric fission as shown in Fig. 8 except energy scale has been extended to 300 Mev. Calculation of the solid-line tail above 24 Mev is according to Eq. (11) as explained in the text. The dashed line shows the minimum symmetric fission cross section consistent with the data of Fig. 7.

where $\bar{\sigma}_a$ and $\bar{\sigma}_s$ are the average cross sections in the energy range 24 to E_0. In this equation the integrals can be calculated from our cross sections to 24 Mev and the Schiff[24] thin-target spectrum properly normalized.[10] $R(E_0)$ is known from the data of Schmitt and Sugarman as shown in Fig. 7. This leaves two unknowns, $\bar{\sigma}_a$ and $\bar{\sigma}_s$, and only one equation. However, their ratio can be found to a good degree of accuracy if we extrapolate the graph of Fig. 10 to a high energy (we used the curve with $\Phi=5.1$). For the first calculation we chose $E_0=29$ Mev and, by making use of the average cross section so obtained, it was next possible to calculate the average cross sections in the energy range 29–35 Mev. This process was repeated in steps of increasing size to 300 Mev. These cross-section curves are shown in Figs. 9 and 11. In Fig. 9 the tail on σ_a is indicated by the solid line. It decreases slowly from 0.3 millibarn at 35 Mev

TABLE III. Ratio of peak-to-valley cross section as a function of nuclear excitation for various uranium isotopes.

E Mev	Compound nucleus	Ratio peak/valley	Nuclear reaction	Reference
6.50	U^{236}	550	U^{235}+thermal neutrons	a
6.74	U^{234}	400	U^{233}+thermal neutrons	b
6.9	U^{236}	360	U^{235}+0.4-Mev neutrons	c
7.7	U^{236}	320	U^{235}+1.2-Mev neutrons	c
7.6	U^{239}	200	U^{238}+2.8-Mev neutrons	d
12–24	U^{238}	25–2.7	$U^{238}+h\nu$	this paper

[a] E. P. Steinberg and M. S. Freedman, Paper 219, reference 11.
[b] Steinberg, Seiber, Goldstein, and Dudley, U. S. Atomic Energy Commission declassified document MDDC-1632, Jan. 6, 1948 (unpublished).
[c] P. W. Spencer, Brookhaven National Laboratory Conference Report BNL-C-9, July, 1949 (unpublished).
[d] Kebler, Steinberg, and Glendenin, Phys. Rev. 94, 969 (1954).

[24] L. I. Schiff, Phys. Rev. 83, 252 (1951).

to 0.1 millibarn at 300 Mev. The initial portion of the symmetric-fission cross-section tail is shown in Fig. 8 and the whole curve to 300 Mev is shown in Fig. 11. This cross section falls to approximately 0.2 millibarn at 25 Mev then rises reaching a value at 300 Mev nearly equal to the low-energy peak cross section. The two cross sections are equal at ~50 Mev, with σ_s becoming larger at the higher energies.

To get a lower limit to the magnitude of the large symmetric-fission cross-section tail, we can assume $\bar{\sigma}_a$ in Eq. (11) to be zero at all energies above 24 Mev and repeat the previous calculations. The results of such calculations is indicated by the dashed lines in Figs. 8 and 11. This is the minimum $\bar{\sigma}_s$ value consistant with experimental data and is not much different from our previous results.

At this point we wish to emphasize one fact. The σ_a and σ_s cross sections are given as functions of the *energy of excitation of the compound nucleus, not the energy of excitation when fission occurred.* These two energies are not necessarily equal since the compound nucleus may lose a considerable amount of its excitation energy by multiple neutron emission[1,25] prior to fissioning. In fact, the tail on the asymmetric fission curve, if it really exists, may simply indicate that some nuclei have become de-excited by multiple neutron emission to such an extent that fission really occurred at low energy. Similarly, the rise in the symmetric fission cross section curve above 25 Mev may indicate the appearance of a fast mode of fission which competes effectively with neutron emission, resulting in a larger fraction of the excited nuclei fissioning while still retaining a considerable portion of this energy of excitation.

3-DIMENSIONAL SHAPE OF THE PHOTOFISSION CROSS-SECTION SURFACE

Cuts at constant mass number through the 3-dimensional $S(Y,A,E_0)$ surface which was constructed from Figs. 1 to 6, gave a number of yield curves similar to these shown in Figs. 1 and 2, but at different mass numbers. These yield curves were solved by the photon difference method to give a number of $(\sigma_{\gamma f}(h\nu))_A$ cross sections curves. Finally, these curves were combined with those already discussed to define the $S(\sigma,A,h\nu)$ surface shown in Fig. 12.

Logarithmic scales were used for the cross section and energy axes of Fig. 12 in order to give the various parts of the surface proper balance. Only the heavy-mass side of $S(\sigma,A,h\nu)$ lying within the energy range 10 to 300 Mev is shown in this figure. The cuts through this surface at $A=117.5$ and $A=139$ are reproductions of the cross sections shown in Figs. 11 and 9 respectively. (Curve at mass number 139 is drawn with the high-energy tail.) None of the cross sections for the other mass numbers which were used to establish the shape of this surface are shown on the figure since to include them would have complicated the drawing.

[25] M. Lindner and R. N. Osborne, Phys. Rev. **94**, 1323 (1954).

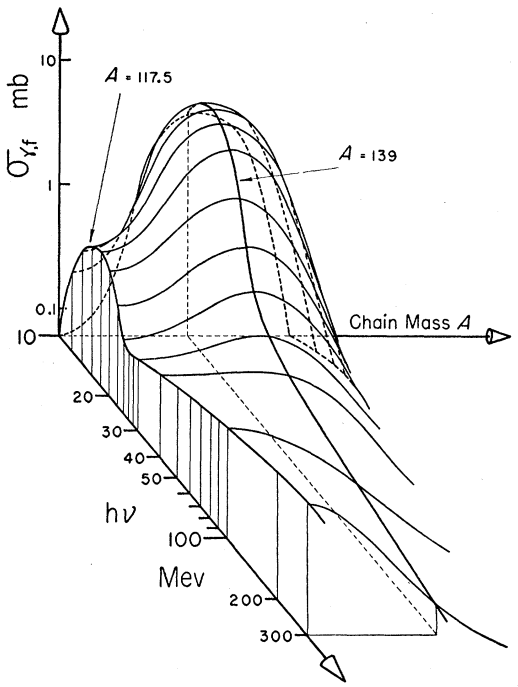

FIG. 12. The $S(\sigma,A,h\nu)$ surface. Since it is symmetric about mass number 117.5, only the higher mass side is shown. The cross sections shown in Figs. 9 and 11 are reproduced on this surface as curves at mass numbers 139 and 117.5 respectively. Note that the energy scale starts at 10 Mev on the low-energy side so that the $A=139$ curve cuts the $\sigma-A$ plane at a finite value. The shape of this surface to 24 Mev is quite well established and above this energy only the $A=117.5$ curve is known with any accuracy.

It must be pointed out that in the high-energy region only the symmetric cross section has been established with any degree of accuracy, the asymmetric cross section is known to an order of magnitude, and nothing is known of the high-energy photofission cross sections for other mass numbers.[26] From these meager data we can, however, conclude that the high-energy photofission cross section is symmetric in mass at constant photon energy, and from the analysis by Schmitt and Sugarman of their data we can take this curve to have a width at half-maximum of ~20 mass units.

TOTAL PHOTOFISSION CROSS SECTION

There are two methods by which the total photofission cross section can be calculated: (i) The total yield at any betatron energy E_0 can be calculated according to Eq. (6) and the cross section can thus be calculated from Eq. (7) by the photon difference method. (ii) According to Eq. (8), this cross section can be obtained at any energy $h\nu$ by taking the area under the curve defined by a cut in the surface of Fig. 12 at that energy.

[26] It was not possible to calculate the high-energy cross-section tails for these intermediate mass numbers from a yield curve extending to high energy, because the cross section so obtained is very sensitive to the absolute photon dose delivered to the sample at each energy. The calculation of σ_a and σ_s was made possible through the availability of the ratio of yields which are not dependent on the irradiation dose.

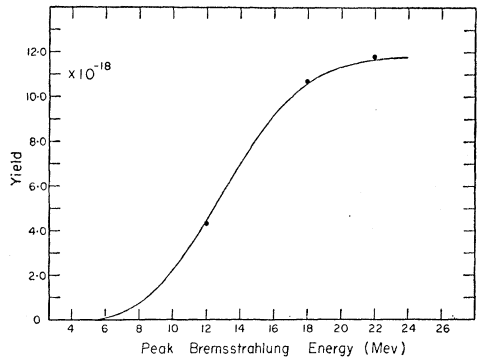

FIG. 13. Total fission yield curve. The 3 points represent the areas under the curves of Figs. 3, 4, and 5. It is found that each of these 3 points is 18.4 times the corresponding yields on Fig. 2 and this curve was drawn similar to it.

The first method was used to calculate the total photofission cross section in the low-energy region (to 24 Mev), and the second method was used to estimate the magnitude of this cross section at high energy.

Graphical integration of the areas under each of the mass-yield curves shown in Figs. 3, 4, and 5 gave three points on the total fission yield curve. The 3 areas are somewhat dependent on the precise shapes chosen for the peaks of the mass-yield curves, particularly the fine structure "hump." Since it has been established experimentally[6] that the shape of the peaks does not vary appreciably with energy, all 3 curves were drawn with the same peak shapes to within the limitations set by our experimental points. Because the area under the trough contributes very little to the total area under each curve, it would appear that the total fission yield should be closely proportional to the yield of mass 139. This was found to be true and the area in each case was found to be 18.4 times the yield of mass chain 139.

The total mass-yield curve is shown in Fig. 13 with the 3 points at 12, 18, and 22 Mev obtained by the graphical integration indicated by circles. Since this curve is identical with that for mass chain 139 shown in Fig. 2 except for the factor 18.4, the total photofission cross section, $\sigma_{\gamma f}$, to 24 Mev can be obtained directly from Fig. 9 by multiplying it by this factor. The resultant curve so obtained is shown in Fig. 14. It has a peak value of 125 millibarns at 14 Mev and an integrated cross section to 24 Mev of 1.1-Mev barns. The width at half-maximum is 8.8 Mev. These values are in good agreement with the measurements of Duffield and Huizenga.[5] They report a peak cross section of 180 millibarns situated at 14 Mev and an integrated cross section to 20 Mev of 1.2-Mev barns.

Above 150 Mev we can obtain the total photofission cross section from our values of σ_s and the estimate by Schmitt and Sugarman[6] that it has a half-width of 21 mass units. Above 150 Mev σ_s is quite constant $\sim$0.65 millibarn (see Fig. 11). We thus find $\sigma_{\gamma f}$ in this energy region to be $\sim$7 millibarn. This is in surprisingly good agreement with the average value of 7 millibarn found by Schmitt and Sugarman.[6] Below 150 Mev the symmetric cross section decreases with decreasing energy; however, the asymmetric cross section probably becomes more important, and as a first approximation we can estimate the total photofission cross section to remain constant.

Levinger and Bethe[27] and more recently Gell-Mann, Goldberger, and Thirring[28] have shown that the integrated nuclear absorption cross section for photons of all multipolarities is given by

$$\int_0^{\mu} \sigma_c dh\nu = 0.060 \frac{ZN}{A}\left(1+0.1\frac{A^2}{ZN}\right), \qquad (12)$$

where μ is the meson threshold $\sim$150 Mev, σ_c is the photon capture cross section, and the other symbols are as usually defined. For U^{238} this equation gives an integrated cross section of 4.8 Mev barn. From the above analysis we can estimate the integrated total photofission cross section to 150 Mev to be 1.2 Mev barns. Duffield and Huizenga measured the integrated (γ,n) cross section in U^{238} to 20 Mev and find it to be 2.6 Mev barns. The difference of 1.0 Mev barn between the sum of these two experimental values and 4.8 Mev barns may represent the high-energy tail on the (γ,n) cross section as well as contributions from the $(\gamma,2n)$, (γ,np), (γ,p), etc., reactions.

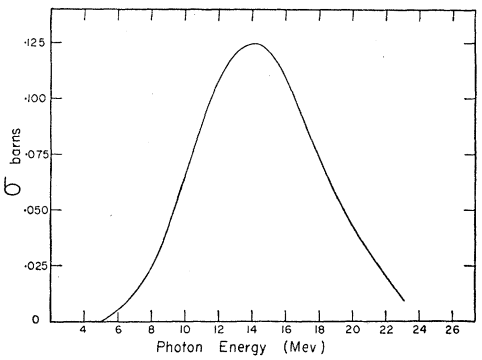

FIG. 14. Total photofission cross section as a function of photon energy. This curve can be obtained from Fig. 13 by the photon difference method, or since Fig. 13 is similar to Fig. 2 then this cross section is similar to that of Fig. 9 except that each ordinate is 18.4 times larger.

The authors would like to thank the Canadian National Research Council for financial assistance in the form of grants, and for scholarships to T.M.K. and A.G.W.C. They would also like to thank E. C. B. Pederson and H. J. King for analyzing some of the decay curves and Miss E. Shmyr and Miss R. Krehbiel for analytical assistance.

[27] J. Levinger and H. A. Bethe, Phys. Rev. **78**, 115 (1950).
[28] Gell-Mann, Goldberger, and Thirring, Phys. Rev. **95**, 1612 (1954).